applied sciences

MDPI

Article

Impact of the Polishing Suspension Concentration on Laser Damage of Classically Manufactured and Plasma Post-Processed Zinc Crown Glass Surfaces

Christoph Gerhard [1,*] and Marco Stappenbeck [2]

[1] Faculty of Engineering and Natural Sciences, Technical University of Applied Sciences Wildau, Hochschulring 1, 15745 Wildau, Germany
[2] Faculty of Natural Sciences and Technology, University of Applied Sciences and Arts, Von-Ossietzky-Straße 99, 37085 Göttingen, Germany; marco.stappenbeck@hawk-hhg.de
* Correspondence: christoph.gerhard@th-wildau.de; Tel.: +49-3375-508-231

Received: 2 August 2018; Accepted: 31 August 2018; Published: 4 September 2018

Featured Application: The specific application of the presented work is the increase in laser-induced damage threshold of polished components made of optical glasses such as lenses, prisms, and protection windows.

Abstract: The laser-induced damage threshold of optics is an issue of essential importance in high-power laser applications. However, the complex and partially interacting mechanisms as well as the underlying reasons for laser damage of glass surfaces are not yet fully understood. The aim of the present work is to contribute to a better understanding of such damage mechanisms by providing original results on the impact of classical glass surface machining on the laser-induced damage threshold. For this purpose, glass samples were prepared with well-defined process conditions in terms of the used lapping and polishing agents and suspensions. Further, the samples were post-processed by atmospheric pressure plasma for precision cleaning. The laser-induced damage threshold and surface contamination by residues from the manufacturing process were determined before and after plasma post-processing. It is shown that the polishing suspension concentration has a certain impact on the laser-induced damage threshold and surface contamination by residues from used working materials. The highest damage threshold of 15.2 J/cm^2 is found for the lowest surface contamination by carbon which occurs in the case of the highest polishing suspension concentration. After plasma treatment for merely 60 s, this value was increased to 20.3 J/cm^2 due to the removal of surface-adherent carbon. The results thus imply that the laser-induced damage threshold can notably be increased by first choosing appropriate process parameters during classical manufacturing and second plasma post-processing for surface finishing.

Keywords: polishing; glass; optics manufacturing; surface contamination; laser-induced damage threshold; plasma cleaning

1. Introduction

Optical components with high laser-induced damage threshold (LIDT) are of essential importance for the realisation of optical systems used for high-power laser setups and facilities. However, classically manufactured optics exhibit comparatively poor laser resistance which can be directly attributed to effects arising in the course of different optics manufacturing process steps. Conventional optical manufacturing involves rough grinding, fine grinding or lapping, and polishing. By these steps, material removal is achieved by the application of different abrasives where the mechanical impact of such abrasives on the glass surface comes along with the formation of either open or closed subsurface

micro cracks as shown in Figure 1. The crack depth is approximately 0.3 times the mean diameter of the used abrasive grains and ranges from 1 to 20 µm for polished surfaces [1]. Such cracks were identified to play a key role for laser damage due to the formation of interference effects, an increased absorption and a reduction in mechanical strength of a glass surface [2,3]. Moreover, residues from operation materials used in optics manufacturing can accumulate within existing micro cracks [4]. This leads to a complex possible contamination consisting of (i) mineral oil-containing cooling lubricants used during rough grinding, (ii) wear debris from abrasive grains, e.g., silicon carbide (SiC) or diamond (C) from the rough and fine grinding or lapping process, and (iii) polishing agents as for example cerium oxide, zirconium oxide, or aluminium oxide as well as wear debris from the used polishing pad.

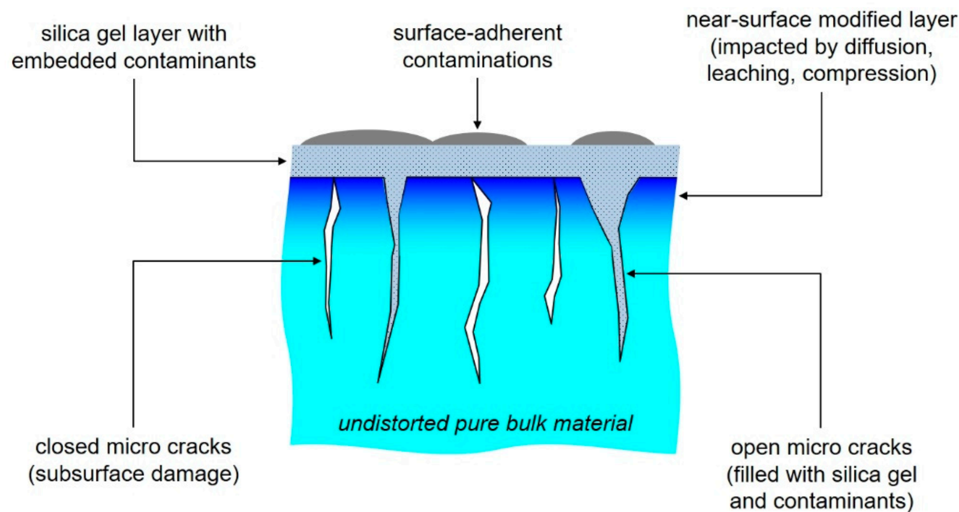

Figure 1. Overview on possible defects of classically manufactured silicon dioxide-based glass surfaces [5].

Since cooling lubricants and lapping and polishing suspensions are water-based operating materials, the involved hydrogen further impacts the glass surface, for example by hydrolytic scission. This leads to the formation of silica gel or hydrated silica during mechanical chemical polishing (MCP) in the case of silicon dioxide-based glasses [6]. As shown in Figure 1, this medium further accumulates within cracks, roughness valleys and digs and can act as matrix for the above-mentioned contaminants and preferentially residues from polishing agents as shown by *Liao* and co-workers [7]. Moreover, it was recently reported that an accumulation of such residues within surface and subsurface damage, e.g., micro cracks, gives rise to surface inhomogeneity in terms of chemical composition [4,8]. These residues or contaminants act as precursors for laser damage [9–11] and consequently reduce the LIDT of polished glass surfaces [12]. Against this background, a considerable number of investigations on surface and subsurface contamination by polishing agents were performed in the past, e.g., [7,9,13,14]. *Krol* and co-workers have further shown that the LIDT of fused silica depends on the polishing method and the particularly corresponding density of such precursors, respectively [15]. It is further known that severe reduction in LIDT also results from surface contamination by carbonaceous compounds [16]. For instance, *Bien-Aimé* and co-workers have shown that organic contaminants, here the hydrocarbon dioctylphthalate (DOP), can lower the LIDT dramatically [17]. In practice, optics surfaces may exhibit severe carbon contamination [18] which might result from the use of carbon-based cleaning agents such as ethanol (C_2H_6O) or acetone (C_3H_6O) or originate from adsorption of hydrocarbons from ambient air in the course of storing or usage [19].

In order to increase the LIDT of optics surfaces, different approaches and techniques for monitoring, controlling, and removing surface contaminants were investigated and developed in the past [20,21]. This includes different post-processing steps after classical polishing such as carbon

dioxide laser treatment [22], hydrofluoric acid (HF) etching [1], ion beam etching (IBE) [23] or the combination of HF etching, subsequent precision polishing and final ion beam etching [24,25]. In the first case, an increase in LIDT is mainly due to surface relaxation via laser melting whereas the application of etching techniques allows the removal of polishing compounds, metal impurities and subsurface damages [26].

The latter issue can efficiently be addressed with the aid of plasmas. As shown by *Juškevičius* and co-workers, the removal of near-surface layers—and subsurface damage, respectively—with a thickness in the range from 50 to 200 nm via etching by argon radio frequency plasma in vacuum allows a significant increase in LIDT of fused silica surfaces by a factor of 8.4 [27]. Moreover, *Zhang* and co-workers have successfully applied oxygen plasmas for reducing the number of micro surface defects on zirconium dioxide films. Thanks to such surface healing, the LIDT was increased by a factor of 1.45 (from 15.9 J/cm^2 to 23.1 J/cm^2) [28] due to the reduction in absorption of incoming laser irradiation. However, further work by the authors on hafnium dioxide films showed that oxygen plasma treatment may also not impact the LIDT if subsurface nanoscale absorber defects are not affected or removed by the plasma [29].

A special type of absorber defects contributing to a decrease in LIDT are surface-adherent carbonaceous compounds as mentioned above. In this context, atmospheric pressure plasmas have turned out to be suitable and powerful tools for surface cleaning [18,30–32]. Most recently, it was shown that the use of direct dielectric barrier discharge (DBD) plasmas at atmospheric pressure using argon as process gas allows an increase in LIDT of super-polished sapphire window surfaces by a factor of 1.5 (from 7.84 J/cm^2 to 11.89 J/cm^2) [16]. This effect is not due to surface etching or material removal but selective removal of surface-adherent contaminants by plasma species. Against this background, the impact of such plasma treatment on zinc crown glass samples was investigated in the present work. Moreover, special attention was also paid to the influence of process parameters applied during sample preparation, namely the particular polishing suspension concentration.

2. Materials and Methods

2.1. Sample Preparation

In this work, plane samples made of zinc crown glass (glass type N-ZK7 from Schott AG, Mainz, Germany) were investigated. The samples were produced by classical optical manufacturing via rough grinding, fine grinding and polishing as described in more detail in [33]. For fine grinding, the method of loose abrasive grinding, also referred to as lapping, was applied. Here, a lapping suspension consisting of water and silicon carbide abrasives with a grain size in the range from 2 to 14 μm (F800 FEPA standard) was used. As usual in optics manufacturing, the samples were lapped slightly concave in order to ensure edge support of the tool employed in the subsequent and final manufacturing step, polishing. For this step, a plane polishing tool with a polishing pad made of polyurethane was used since this type of polishing pad allows reducing the number of micro cracks formed during polishing [34]. The polishing agent was a premixed water-based polishing suspension (type Hastilite PO from Universal Photonics, Inc., NY, USA), where the actual polishing agent is cerium oxide (CeO_2) with a mean grain size of 0.8 μm. The initial concentration of this premixed polishing suspension was c_s = 60%. In order to obtain further polishing suspensions with defined concentrations, the premixed suspension was thinned down using distilled water. According to

$$c_s = \frac{m_{pa}}{m_s} \cdot 100\%, \tag{1}$$

where m_{pa} is the mass of the polishing agent within the suspension and m_s is its total mass [33], two further suspensions with a concentration of c_s = 44% and c_s = 19%, respectively, were realised in this way.

2.2. Measurement Techniques and Approaches

In order to determine the LIDT, a diameter regression fit method as suggest by *Liu* [35] was applied. This 1-on-1 laser damage testing approach is an easy and distinct method for the determination of the LIDT in the picosecond pulse duration range on the basis of the diameter of ablated spots [36]. Here, the sample surface is sectioned into a number of test sites and each site is irradiated with a single laser pulse with a defined and known fluence. The squared diameters of the damaged sites are then plotted vs. the laser fluence. The resulting straight line is extrapolated and the intercept of this regression line with the logarithmically scaled *x*-axis (i.e., the fluence values) finally gives the LIDT as shown schematically in Figure 2.

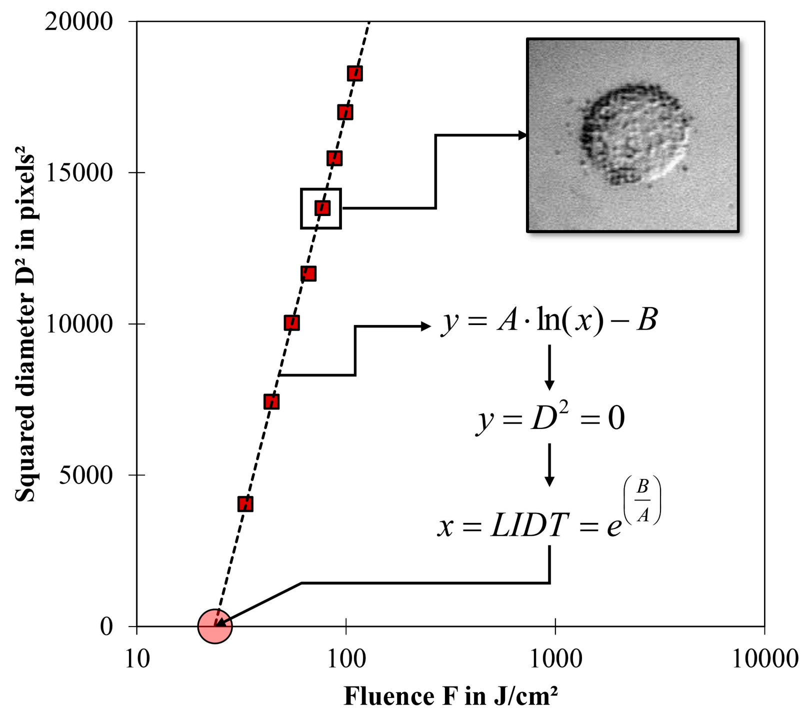

Figure 2. Principle of the diameter regression technique applied for the determination of the laser-induced damage threshold (LIDT) including an example for the observed damage morphology (inset).

In the present case, 25 test sites per sample were investigated. The used laser source was a Yb:YAG solid state picosecond laser (model TruMicro 5025 from Trumpf GmbH & Co. KG, Ditzingen, Germany) with a pulse duration of τ = 8 ps, an emission wavelength of λ = 1030 nm, and a maximum pulse energy of E = 125 µJ. The raw beam with a diameter of $2w_r$ = 5 mm was focused onto the sample surface by a convex lens with a focal length of f = 50 mm, resulting in a laser beam waist diameter of $2w_0$ = 17 µm. As a consequence, the initial laser fluence at the maximum pulse energy was 110 J/cm^2. This value was successively reduced in eight steps down to a minimum fluence of 22 J/cm^2 where the decrement per step was 11 J/cm^2. For the determination of the actual LIDT, the diameters of the laser-induced damaged sites on the sample surfaces (given in pixels) were measured with the aid of a light microscope (model Axioskop 2 MAT from Carl Zeiss Microscopy GmbH, Jena, Germany).

In addition to the LIDT, the chemical composition of the sample surfaces was measured using a scanning X-ray photoelectron spectroscopy (XPS) apparatus (model PHI VersaProbe II from ULVAC-PHI, Inc., Hagisono, Japan) in order to determine and identify impurities induced by the manufacturing process. Here, the elements of interest were carbon and cerium, representing possible contaminants occurring in the course of sample preparation by rough grinding, lapping and polishing as well as silicon and oxygen since the investigated zinc crown glass is a high-silica glass

(60–70 wt %) [37]. The particular elemental fractions were determined via evaluation of the C1s-peak of carbon, the Ce3d5-peak of cerium, the Si2p-peak of silicon, and the O1s-peak of oxygen in the measured spectrum.

All measurements were performed on samples prepared at three different concentrations of the used polishing agent (19, 44, and 60%, see above). In addition, the impact of a plasma post-processing as described in the following section on the measured parameters was investigated.

2.3. Plasma Post-Processing

For plasma post-processing, a plasma source as described in more detail in previous work [38–40] was used. This plasma source basically consists of a conical rotation-symmetric high-voltage copper electrode embedded in a plastic housing made of polyoxymethylene (POM). The gas channel for feeding the plasma process gas is found between the high-voltage electrode and the housing. In the present work, argon (Ar 5.0 from Linde Gas AG, Munich, Germany) was used as process gas where the gas flow rate was 4 standard litres per minute. The plasma was ignited between the high-voltage electrode and an external plane ground electrode, both made of copper. The glass samples were placed between the high-voltage electrode and the ground electrode; the working distance between the outlet nozzle of the plasma source and the work piece surface was approx. 10 mm. This setup leads to the formation of a direct dielectric barrier discharge (DBD) plasma where the sample itself is an essential part of the plasma ignition which consequently occurs directly on the sample surface as visualised in Figure 3.

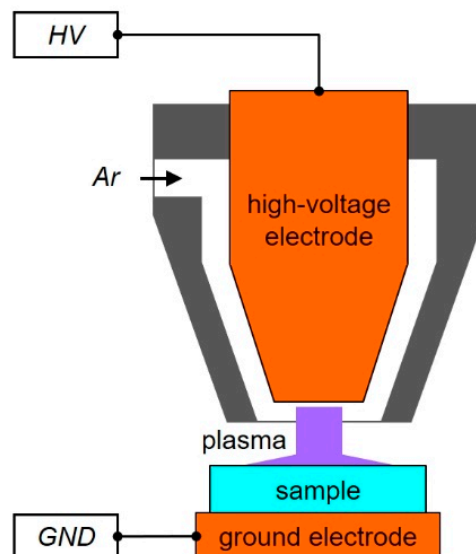

Figure 3. Experimental setup for plasma post-processing of polished glass samples applying a direct dielectric barrier discharge (DBD) plasma.

The plasma source was driven by a pulsed power supply where the voltage of each pulse was U = 11 kV, the nominal pulse repetition rate was f = 7 kHz and the pulse duration of each pulse was τ = 80 µs. Due to the functional principle—the DBD—the plasma gas temperature and sample surface heating, respectively, are quite moderate and amount to approximately 90 °C as determined via infrared camera measurements in previous work [41]. This is due to the fact that extremely low currents in the range of some microamperes to milliamperes occur during DBD plasma operation. In contrast to classical arc discharges, burn-off of the electrode material is moreover reduced or even inhibited, avoiding the deposition of electrode material on the sample surface. In the present work, the plasma treatment duration was 60 s. The impact of such short-term direct DBD plasma post-processing was

investigated since it was observed in previous work that applying this type of plasma for merely one minute allows considerable smoothing of optical media [39,40] as well as surface cleaning and an accompanying increase in LIDT of sapphire substrates [16].

3. Results

3.1. Polished Samples

The investigation of the chemical composition of the samples after polishing revealed that the cerium content was approximately 0.25 ± 0.01 at% for all samples, so no dependency of surface contamination by the polishing agent on the polishing suspension concentration was detected. In contrast, an obvious impact of the polishing suspension concentration on first the surface contamination by carbon, and second the LIDT, was observed as shown in Figure 4.

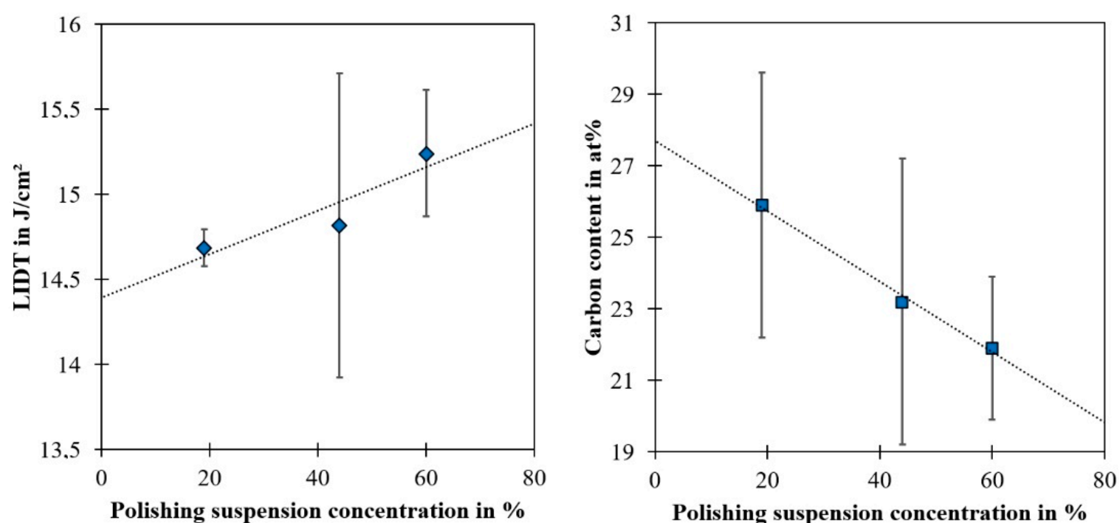

Figure 4. Laser-induced damage threshold (LIDT, **left**) and carbon content (**right**) vs. polishing suspension concentration including trend (dotted line).

It turns out that the LIDT increases with increasing polishing suspension concentration, whereas the carbon content exhibits the reverse behaviour. As a consequence, these two considered parameters indicate a certain correlation; it can be stated that the lower the carbon content, the higher the LIDT. At an average, an LIDT of the polished zinc crown glass of approximately 15 J/cm^2 was determined. This value cannot be compared to literature since the LIDT of this specific glass is not reported. However, it is in a typical range for transparent optical materials exposed to focussed laser irradiation at a wavelength around 1 micron and a pulse duration of some picosconds. For fused silica, quite different values ranging from approximately 5 J/cm^2 [42] to even 44 J/cm^2 [43] are reported. For sapphire, the LIDT amounts to approximately 8 J/cm^2 [16,44]. Finally, dielectric coatings feature LIDT in the range from about 2 to 5 J/cm^2 [45,46].

3.2. Polished and Plasma Post-Processed Samples

As ascertained via XPS measurements, plasma post-processing did not notably impact the cerium content at the sample surfaces. With respect to the initial average value of 0.25 ± 0.01 at%, a marginal increase to 0.26 ± 0.09 at% was detected. In contrast, a significant reduction in carbon content was detected as shown by the comparison in Figure 5. At an average, the carbon content was 23.67 ± 2.04 at% before and 7.82 ± 0.86 at% after plasma post-processing, corresponding to a decrease by a factor of approximately 3.

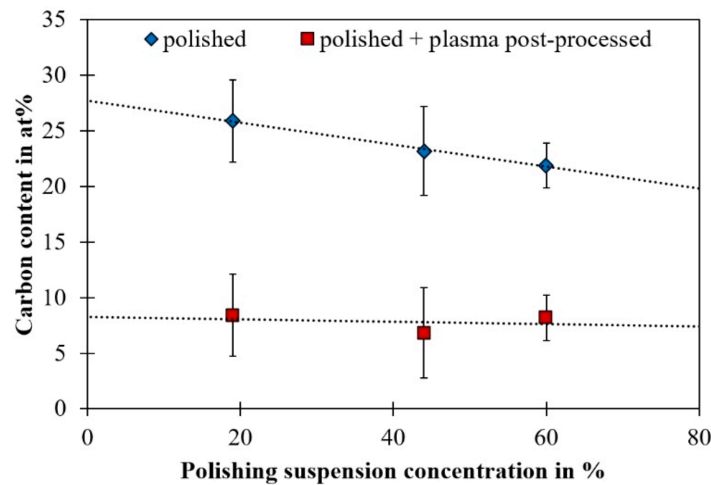

Figure 5. Carbon content of zinc crown glass samples before and after plasma post-processing vs. polishing suspension concentration including trend (dotted line).

It further turns out that, in contrast to the initial state before plasma post-processing, no dependency of the particular carbon content on the polishing suspension concentration is observed after plasma treatment as visualised by the trend lines in Figure 5. The residual carbon content is rather constant. Another observed effect is a general increase in LIDT due to plasma post-processing as shown in Figure 6.

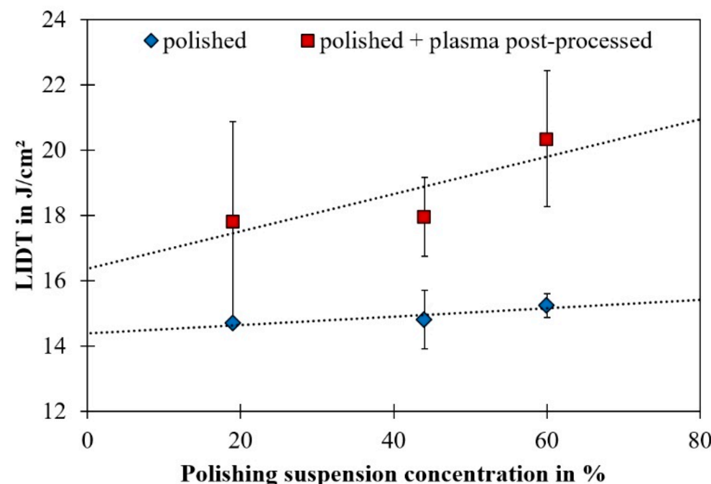

Figure 6. Laser-induced damage threshold (LIDT) of zinc crown glass samples before and after plasma post-processing vs. polishing suspension concentration including trend (dotted line).

In contrast to the carbon content presented in Figure 5, the LIDT shows a slightly stronger dependency by trend on the polishing suspension concentration after plasma post-processing.

4. Discussion

4.1. Impact of the Polishing Suspension Concentration

As a general point, it should be noted that the measurements presented in Section 3 feature relatively large error bars. Regarding the LIDT measurements, statistically distributed absorbing surface defects may in some cases not be affected by the incident laser irradiation due to the small

spot size of the laser focus. This fact might contribute to the relatively large error bars of the LIDT values which result from the particular values measured at 25 test sites per sample. The observed dependencies as discussed in the present subsection have thus to be treated as a general trend.

As presented in Section 3.1, the cerium content at the surfaces of the investigated samples was approximately 0.25 at% after polishing. This value was detected for all polishing suspension concentrations, a correlation between the cerium content within the suspension and surface contamination by this element or polishing agent, respectively, was thus not observed. However, the use of such polishing suspension led to a constant attachment or implantation of cerium at/into the surface as discussed in more detail in Section 4.2. This effect, a saturation of the interaction between the polishing pad or suspension and the glass surface during polishing once a certain concentration of the polishing suspension is reached, was already reported in 2008 by *Rogov* and co-workers [47].

An interesting point is the trend of a decreasing carbon content with increasing polishing suspension concentration. For the origin of the detected carbon, several sources from the manufacturing process should be considered since the glass itself does not contain any carbon according to the manufacturer's datasheet [37]:

- First, the carbon could originate from the rough grinding process which is usually performed with the aid of cylindrical cup wheels where the bound abrasives are usually made of diamond, i.e., pure carbon.
- Second, the application of cooling lubricants during rough grinding is another possible source for carbon since such lubricants are a suspension of water and carbonaceous mineral oil.
- Third, the lapping agent used for sample preparation, silicon carbide (SiC), could accumulate within digs and cracks of the glass surface and finally be embedded within hydrated silica which is formed during polishing as introduced in Section 1. In the course of this terminal production step, carbonaceous contaminants could finally arise in the form of wear debris from the used polishing pad made of polyurethane foil. This last aspect could explain the observed behaviour, i.e., an increased carbon content in the case of thin suspensions. Here, wear preferentially occurs between the polishing pad and the glass surface due to direct contact. The higher the concentration of the suspension, the more polishing agent grains are found in between the pad and the surface, consequently reducing direct wear.

The presence of carbon turns out to be the main reason for a decrease in LIDT. Since the cerium content is quite constant for all polishing suspension concentrations as mentioned in Section 3.1, the impact of this parameter on the LIDT can be assumed to be constant as well. In contrast, the LIDT and the carbon content tends to depend on the polishing suspension concentration, see Figure 4. The increase in LIDT with decreasing carbon content can be explained by the fact that a reduction in surface-adherent carbon and carbonaceous compounds corresponds to a reduction in absorbing contaminants which may act as precursor for laser damage. This is visualised by the comparison of the absorption coefficients of the abovementioned involved media (or a particular reference material) in Table 1. For example, the absorption coefficient of the used lapping agent, silicon carbide, is more than four million times higher than the absorption coefficient of the investigated zinc crown glass.

Table 1. Absorption coefficients of the investigated zinc crown glass, silicon carbide, glycol, and immersion oil at a wavelength of λ = 1030 nm.

Material	Absorption Coefficient α in cm^{-1}	Reference
Zinc crown glass N-ZK7	0.0024	[37]
Silicon carbide [1]	10,070	[48]
Glycol [2]	0.22	[49]
Immersion oil [3]	1.013	[50]

[1] Lapping agent used in this work, [2] reference material for polyurethane (i.e., the polishing pad material used in this work), [3] reference material for mineral oil-based cooling lubricants.

It should be noted that this comparison of the linear absorption coefficients of the investigated glass and possible surface-adherent and subsurface contaminants is only one aspect of laser-induced damage. Especially in the considered pulse duration range of some picoseconds, a number of further effects contribute to the LIDT. This includes nonlinear optical phenomena such as self-focussing, a dynamic increase in absorption due to multiphoton absorption and the formation of charge carriers by laser-induced avalanche ionisation. However, it can finally be stated that the polishing suspension concentration and the polishing process in general may have a noticeable impact on the LIDT. This effect was also qualitatively reported by *Zawilski* and co-workers where the LIDT of optical crystals was increased via optimising the applied polishing process [51].

4.2. Impact of Plasma Post-Processing

As mentioned in Section 3.2, cerium was not removed by plasma post-processing; its content was even slightly increased. This indicates that the detected cerium was not surface-adherent, but implanted within a subsurface zone during polishing. Considering that the information depth of XPS is approximately 10 nm and that the mean thickness of hydrated silica layers is in this order of magnitude (1 to 20 nm [6]), the cerium content measured via XPS was most likely embedded in such a silica layer which was formed in the course of the polishing process. Apparently, this layer was not removed by the short-term plasma treatment due to its chemical stability. The slight increase in cerium content rather indicates a plasma-induced uncovering of this element by the removal of surface-adherent carbonaceous contaminants as discussed in more detail below. It can finally be stated that even though cerium is known to be a precursor for laser damage [12], its impact on the observed increase in LIDT can be neglected in the present case. In contrast, the correlation of the LIDT and the near-surface carbon content is obvious; as shown in Figure 7, the LIDT increases with decreasing carbon content.

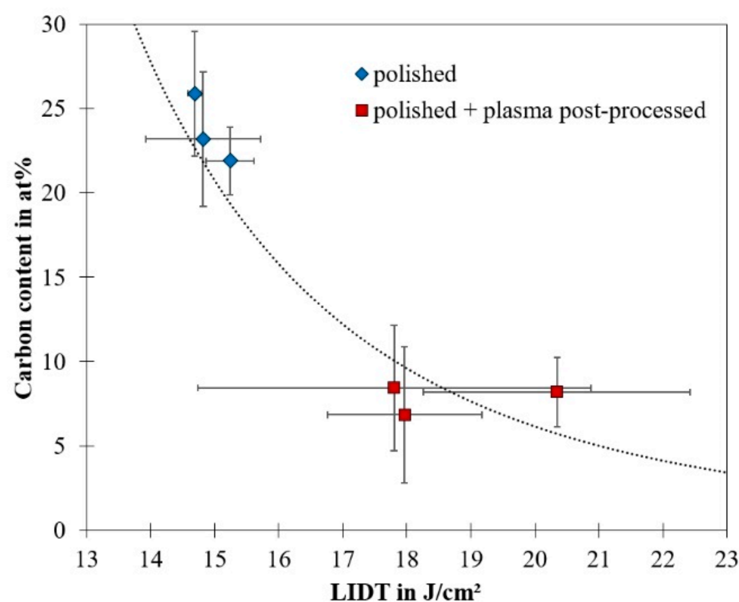

Figure 7. Correlation of the carbon content and the laser-induced damage threshold (LIDT) of polished zinc crown glass samples with and without plasma post-processing including general trend (dotted line).

The impact of the presence of carbon on surface absorption and the resulting LIDT was already discussed in Section 4.1. The removal of carbon by the plasma thus allows reducing the effects and mechanisms mentioned there. Plasmas are well known to be suitable for the removal of surface-adherent hydrocarbons (C_xH_y, where $x < y$) or other carbonaceous compounds. For instance,

decomposition of hydrocarbons can be initiated by atomic oxygen (O) which is provided via dissociation within the plasma volume by collisions of oxygen molecules (O_2) with free electrons. According to

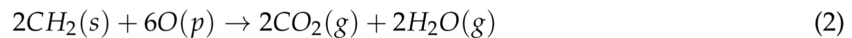

$$2CH_2(s) + 6O(p) \rightarrow 2CO_2(g) + 2H_2O(g) \quad (2)$$

the resulting volatile by-products are then gaseous carbon dioxide (CO_2) and water (H_2O). This process is very efficient when working with "cold" dielectric barrier discharges [52] and when adding marginal fractions of oxygen (i.e., approximately 1 to 2%) to argon as carrier gas [30,31]. In the present case, the plasma is driven at atmospheric pressure without any housing. Oxygen from the surrounding air is thus taken in by the plasma, subsequently mixed with the used argon and finally subject to the electric discharge within the discharge gap between the high voltage electrode and the sample surface.

Apart from such pure chemical plasma-induced reaction of oxygen species with contaminants, further effects could contribute to the removal of carbon and the cleaning process, respectively. *Swain* and co-workers have reported on the increase in LIDT of crown glass due to laser cleaning at low fluence below the ablation threshold. The authors attributed this effect to a removal of absorbers from the glass surface by irradiation-induced desorption [53]. This mechanism could also play a role in the present case. Even though the plasma fluence is quite low, i.e., F_{plasma} = 0.54 J/cm^2 [39,40], the plasma used in this work is ignited directly on the glass surface and thus provides a considerable amount of ultraviolet irradiation which might induce desorption. Another possible underlying mechanism, the emission of electrons or ions from the surface and the resulting alteration of electrical forces within the surface which bind the contaminants, was reported by *Logothetis* and *Hartman* [54]. This effect finally leads to a removal of contaminants. As a result of direct plasma ignition on the sample surface, the impact of charged particles on the surface is very high and might support the removal of carbon as observed in this work.

Plasma-induced surface cleaning by the removal of carbon can also be expressed in the form of surface coverage as shown in Figure 8. Here, the surface coverage as given by the ratio of carbon and the glass component silicon (C/Si) is shown. Silicon was chosen for calculating this ratio since silicon dioxide is the main compound of the investigated glass, representing 60–70 wt % of the entire glass weight [37].

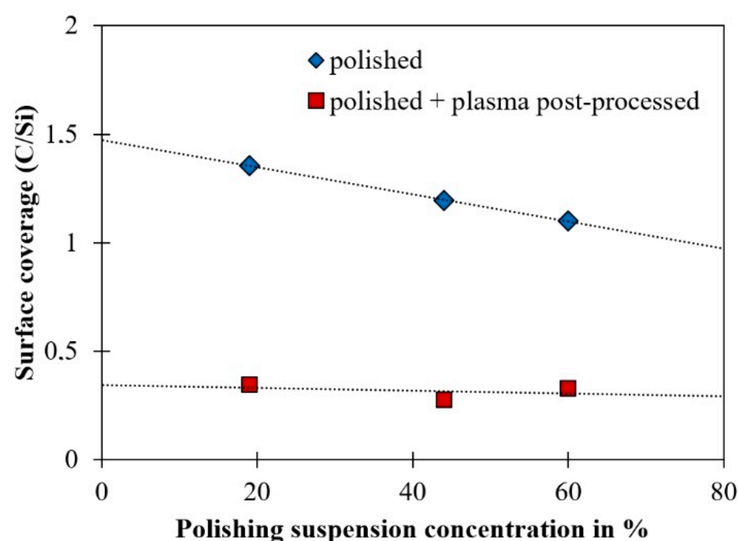

Figure 8. Comparison of the surface coverage by carbon (i.e., the ratio of carbon and silicon) of zinc crown glass samples before and after plasma post-processing vs. polishing suspension concentration including trend (dotted line).

It turns out that a high surface coverage is found for untreated samples where the amount of carbon is even higher than the amount of silicon since the surface coverage value exceeds one in any case. It can further be seen that the degree of surface coverage decreases with increasing polishing suspension concentration (compare also Figure 4). After plasma post-processing, the surface coverage approaches a saturation value of approximately 0.3, corresponding to a total content of carbon of about 7.82% on average. This value does not depend on the initial carbon content before plasma treatment and is thus independent on the polishing suspension concentration. It can consequently be stated that surface-adherent carbon was efficiently removed in all cases in the course of plasma post-processing. However, there is a residual constant carbon content which was not removed by the plasma. It can be assumed that this remaining carbon is given by contaminants from the used tools and working materials which have accumulated within digs and micro cracks underneath and/or within the hydrated silica gel layer. The plasma is thus capable of removing surface-adherent contamination by carbon such as wear debris from the polyurethane polishing pad or residues from cleaning agents but does not affect deeper regions of the polished glass surface.

Even though the final amount of remaining carbon after plasma post-processing does not depend on the initial carbon content, the LIDT shows a certain dependency on this value and the polishing suspension concentration, respectively, where the LIDT increases with increasing polishing suspension concentration. This indicates that the observed increase in LIDT does not exclusively follow from plasma-induced removal of surface-adherent carbon, but further subsurface effects and mechanisms are involved additionally. Such possible mechanisms are constructive interference of incident laser light, an increased absorption and a reduced mechanical strength of the glass due to the presence of micro cracks [3] where absorbing and scattering residues from working materials can moreover accumulate [4]. It is known that the crack density increases with increasing polishing suspension concentration [55]. It can thus be assumed that the crack depth features the same behaviour since, in the case of increasing polishing suspension concentration, the high number of polishing grains between the polishing pad and the glass surface leads to a reduction in local pressure and load. Consequently, surface stress as expressed by the stress intensity factor K is reduced as shown by *Swain* and co-workers [56]. Since this factor is inversely proportional to the crack depth [57], a higher crack depth and crack volume arise in this case, so the available volume for the accumulation of laser light-absorbing contaminants is increased. Based on this theoretical approach, the LIDT should finally feature a systematic dependency on the polishing suspension concentration. A trend towards this behaviour was observed in the present work, see Figure 4. One has to consider that this dependency was not only observed for polished and plasma post-processed samples, but also for polished ones, see Figure 6. This fact supports the assumption that the polishing suspension concentration and the resulting crack density may play an additional and essential role for the observed behaviour of the LIDT.

5. Conclusions

The results presented in this work clearly show that the laser-induced damage threshold of the investigated glass is directly related to surface contamination by carbon. The highest LIDT was found for the lowest contamination which occurred in the case of the highest polishing suspension concentration. In contrast, surface contamination by the actual polishing agent, cerium, does not depend on the polishing suspension concentration. The results thus suggest that classical polishing of laser optics surfaces with high polishing suspension concentration allows increasing the LIDT. However, this assumption has to be verified in the frame of further ongoing investigations due to the extraordinarily high number of possible configurations during manufacturing in terms of the glass type, the used abrasives (especially carbon-based ones such as silicon carbide or diamond), the pH-value of the polishing suspension, the used tools and polishing pads, etc.

The increase in carbon contamination with decreasing polishing suspension concentration is most likely due to a higher wear between the polishing pad made of carbonaceous polyurethane

and the glass surface, due to a reduced number of polishing grains within the suspension. Thus, the effective direct contact area of the pad and the glass is bigger, consequently leading to increased formation of carbonaceous wear debris from the polishing pad according to the Preston equation [6]. Such debris can adhere on the surface and also accumulate in the formed silica layer or even penetrate into the glass bulk material by diffusion. In this context, the pH-value of the polishing suspension gains importance [58]. This value moreover influences the magnitude of near-surface forces during polishing [59] and the accompanying wear and formation of wear debris. As mentioned above, this point is thus to be investigated in future work.

Apart from an increased carbon contamination, another possible mechanism for the decrease in LIDT with decreasing polishing suspension concentration could be material densification due to local load induced by the polishing tool. Such densification leads to an increase in index of refraction [60] and absorption, respectively. Actually, such an increase in index of refraction with decreasing polishing suspension concentration was qualitatively observed and verified by ellipsometric measurements.

The significant increase in LIDT after plasma post-processing is obviously directly related to the removal of carbon from the glass surfaces. The effect of plasma-induced cleaning of glass by the removal of carbonic contaminations surfaces is well-known and used in quite different fields of application [30]. However, the use of plasmas for increasing the LIDT of optics is a comparatively new area of research (compare Section 1). Plasma post-processing as presented in this work stands out due to the operation at atmospheric pressure and comparatively low temperature, the use of the standard process gas argon and the short treatment duration of 60 s. This approach can be integrated into existing optics production chains quite easily and thus features high potential for industrial processes for surface finishing of high-power laser optics.

Author Contributions: C.G. conceived and designed the experiments, analysed the data and wrote the paper; M.S. prepared the samples, performed the experiments and analysed the data.

Funding: This research received no external funding.

Acknowledgments: The authors thank the German Research Foundation (Deutsche Forschungsgemeinschaft, DFG) and the Ministry for Science and Culture of Lower Saxony (Ministerium für Wissenschaft und Kultur, MWK) for funding the laser source which was used for LIDT measurements. Further, the authors thank Lutz Müller, Robert Köhler, and Daniel Tasche from the University of Applied Sciences and Arts in Göttingen for their help during the preparation and analysis of the investigated samples. In addition, the support by the German Research Foundation (Deutsche Forschungsgemeinschaft, DFG) and the Technical University of Applied Sciences Wildau for covering open access publication costs is gratefully acknowledged.

Conflicts of Interest: The authors declare no conflict of interest. The founding sponsors had no role in the design of the study; in the collection, analyses, or interpretation of data; in the writing of the manuscript, and in the decision to publish the results.

References

1. Suratwala, T.I.; Miller, P.E.; Bude, J.D.; Steele, W.A.; Shen, N.; Monticelli, M.V.; Feit, M.D.; Laurence, T.A.; Norton, M.A.; Carr, C.W.; et al. HF-based etching processes for improving laser damage resistance of fused silica optical surfaces. *J. Am. Ceram. Soc.* **2011**, *94*, 416–428. [CrossRef]
2. Bloembergen, N. Role of cracks, pores, and absorbing inclusions on laser induced damage threshold at surfaces of transparent dielectrics. *Appl. Opt.* **1973**, *12*, 661–664. [CrossRef] [PubMed]
3. Feit, M.D.; Rubenchik, A.M. Influence of subsurface cracks on laser-induced surface damage. *Proc. SPIE* **2004**, *5273*, 264–272. [CrossRef]
4. Pfiffer, M.; Longuet, J.-L.; Labrugère, C.; Fargin, E.; Bousquet, B.; Dussauze, M.; Lambert, S.; Cormont, P.; Néauport, J. Characterization of the polishing-induced contamination of fused silica optics. *J. Am. Ceram. Soc.* **2017**, *100*, 96–107. [CrossRef]
5. Ye, X.; Huang, J.; Liu, H.; Geng, F.; Sun, L.; Jiang, X.; Wu, W.; Qiao, L.; Zu, X.; Zheng, W. Advanced mitigation process (AMP) for improving laser damage threshold of fused silica optics. *Sci. Rep.* **2016**, *6*, 31111. [CrossRef] [PubMed]
6. Cook, L.M. Chemical processes in glass polishing. *J. Non-Cryst. Solids* **1990**, *120*, 152–171. [CrossRef]

7. Liao, D.; Chen, X.; Tang, C.; Xie, R.; Zhang, Z. Characteristics of hydrolyzed layer and contamination on fused silica induced during polishing. *Ceram. Int.* **2014**, *40*, 4479–4483. [CrossRef]
8. Gerhard, C.; Tasche, D.; Uteza, O.; Hermann, J. Investigation of nonuniform surface properties of classically-manufactured fused silica windows. *Appl. Opt.* **2017**, *56*, 7427–7434. [CrossRef] [PubMed]
9. Camp, D.W.; Kozlowski, M.R.; Sheehan, L.M.; Nichols, M.A.; Dovik, M.; Raether, R.G.; Thomas, I.M. Subsurface damage and polishing compound affect the 355-nm laser damage threshold of fused silica surfaces. *Proc. SPIE* **1998**, *3244*, 356–364. [CrossRef]
10. Bertussi, B.; Natoli, J.Y.; Commandre, M. Effect of polishing process on silica surface laser-induced damage threshold at 355 nm. *Opt. Commun.* **2004**, *242*, 227–231. [CrossRef]
11. Krol, H.; Gallais, L.; Grèzes-Besset, C.; Natoli, J.-Y.; Commandré, M. Investigation of nanoprecursors threshold distribution in laser-damage testing. *Opt. Commun.* **2005**, *256*, 184–189. [CrossRef]
12. Neauport, J.; Lamaignere, L.; Bercegol, H.; Pilon, F.; Birolleau, J.-C. Polishing-induced contamination of fused silica optics and laser-induced damage density at 351 nm. *Opt. Express* **2005**, *13*, 10163–10171. [CrossRef] [PubMed]
13. Kozlowski, M.R.; Carr, J.; Hutcheon, I.D.; Torres, R.A.; Sheehan, L.M.; Camp, D.W.; Yan, M. Depth profiling of polishing-induced contamination on fused silica surfaces. *Proc. SPIE* **1998**, *3244*, 365–375. [CrossRef]
14. Bude, J.; Miller, P.; Baxamusa, S.; Shen, N.; Laurence, T.; Steele, W.; Suratwala, T.; Wong, L.; Carr, W.; Cross, D.; et al. High fluence laser damage precursors and their mitigation in fused silica. *Opt. Express* **2014**, *22*, 5839–5851. [CrossRef] [PubMed]
15. Krol, H.; Gallais, L.; Commandré, M.; Grèzes-Besset, C.; Torricini, D.; Lagier, G. LIDT improvement of multilayer coatings by accurate analysis of fabrication steps. *Proc. SPIE* **2005**, *5963*, 596311. [CrossRef]
16. Gerhard, C.; Tasche, D.; Munser, N.; Dyck, H. Increase in nanosecond laser-induced damage threshold of sapphire windows by means of direct dielectric barrier discharge plasma treatment. *Opt. Lett.* **2017**, *42*, 49–52. [CrossRef] [PubMed]
17. Bien-Aimé, K.; Néauport, J.; Tovena-Pecault, I.; Fargin, E.; Labrugère, C.; Belin, C.; Couzi, M. Laser induced damage of fused silica polished optics due to a droplet forming organic contaminant. *Appl. Opt.* **2009**, *48*, 2228–2235. [CrossRef] [PubMed]
18. Gerhard, C.; Weihs, T.; Tasche, D.; Brückner, S.; Wieneke, S.; Viöl, W. Atmospheric pressure plasma treatment of fused silica, related surface and near-surface effects and applications. *Plasma Chem. Plasma Process.* **2013**, *33*, 895–905. [CrossRef]
19. Langmuir, I. The adsorption of gases on plane surfaces of glass, mica and platinum. *J. Am. Chem. Soc.* **1918**, *40*, 1361–1403. [CrossRef]
20. Giuliano, C.R. Laser-induced damage in transparent dielectrics: Ion beam polishing as a means of increasing surface damage thresholds. *Appl. Phys. Lett.* **1972**, *21*, 39–41. [CrossRef]
21. Cheng, X.; Miao, X.; Wang, H.; Qin, L.; Ye, Y.; He, Q.; Ma, Z.; Zhao, L.; He, S. Surface contaminant control technologies to improve laser damage resistance of optics. *Adv. Cond. Matter Phys.* **2014**, *2014*, 974245. [CrossRef]
22. Temple, P.A.; Lowdermilk, W.H.; Milam, D. Carbon dioxide laser polishing of fused silica surfaces for increased laser-damage resistance at 1064 nm. *Appl. Opt.* **1982**, *21*, 3249–3255. [CrossRef] [PubMed]
23. Xu, S.; Zheng, W.; Yuan, X.; Lv, H.; Zu, X. Recovery of fused silica surface damage resistance by ion beam etching. *Nucl. Instr. Meth. Phys. Res. B* **2008**, *266*, 3370–3374. [CrossRef]
24. Kamimura, T.; Akamatsu, S.; Horibe, H.; Shiba, H.; Motokoshi, S.; Sakamoto, T.; Jitsuno, T.; Okamoto, T.; Yoshida, K. Enhancement of subsurface-damage resistance by removing subsurface damage in fused silica and its dependence on wavelength. *Jpn. J. Appl. Phys.* **2004**, *43*, L1229–L1231. [CrossRef]
25. Kamimura, T.; Akamatsu, S.; Yamamoto, M.; Yamato, I.; Shiba, H.; Motokoshi, S.; Sakamoto, T.; Okamoto, T.; Yoshida, K. Enhancement of surface-damage resistance by removing a subsurface damage in fused silica. In Proceedings of the SPIE Conference 35th Annual Symposium on Optical Materials For High Power Lasers: Boulder Damage Symposium, Boulder, CO, USA, 22–24 September 2003; Volume 5237, pp. 224–250.
26. Liu, H.; Ye, X.; Zhou, X.; Huang, J.; Wang, F.; Zhou, X.; Wu, W.; Jiang, X.; Sui, Z.; Zheng, W. Subsurface defects characterization and laser damage performance of fused silica optics during HF-etched process. *Opt. Mater.* **2014**, *36*, 855–860. [CrossRef]

27. Juškevičius, K.; Buzelis, R.; Abromavičius, G.; Samuilovas, R.; Abbas, S.; Belosludtsev, A.; Drazdys, R.; Kičas, S. Argon plasma etching of fused silica substrates for manufacturing high laser damage resistance optical interference coatings. *Opt. Mater. Express* **2017**, *7*, 3598–3607. [CrossRef]
28. Zhang, D.; Shao, J.; Zhang, D.; Fan, S.; Tan, T.; Fan, Z. Employing oxygen-plasma posttreatment to improve the laser-induced damage threshold of ZrO_2 films prepared by the electron-beam evaporation method. *Opt. Lett.* **2004**, *29*, 2870–2872. [CrossRef] [PubMed]
29. Zhang, D.; Wang, C.; Fan, P.; Cai, X.; Zheng, Z.; Shao, J.; Fan, Z. Influence of plasma treatment on laser-induced damage characters of HfO_2 thin films at 355 nm. *Opt. Express* **2009**, *17*, 8246–8252. [CrossRef] [PubMed]
30. Shun'ko, E.V.; Belkin, V.S. Cleaning properties of atomic oxygen excited to metastable state $2s^2 2p^4 (^1S_0)$. *J. Appl. Phys.* **2007**, *102*, 083304. [CrossRef]
31. Iwasaki, M.; Inui, H.; Matsudaira, Y.; Kano, H.; Yoshida, N.; Ito, M.; Hori, M. Nonequilibrium atmospheric pressure plasma with ultrahigh electron density and high performance for glass surface cleaning. *Appl. Phys. Lett.* **2008**, *92*, 081503. [CrossRef]
32. Buček, A.; Homola, T.; Aranyosiová, M.; Velič, D.; Plecenik, T.; Havel, J.; Stahel, P.; Zahoranová, A. Atmospheric pressure nonequilibrium plasma treatment of glass surface. *Chem. Listy* **2008**, *102*, S1459–S1462.
33. Gerhard, C. *Optics Manufacturing: Components and Systems*, 1st ed.; CRC Taylor & Francis: Boca Raton, FL, USA, 2017; ISBN 978-1-4987-6459-9.
34. Li, Y.; Hou, J.; Xu, Q.; Wang, J.; Yang, W.; Guo, Y. The characteristics of optics polished with a polyurethane pad. *Opt. Express* **2008**, *16*, 10285–10293. [CrossRef] [PubMed]
35. Liu, J.M. Simple technique for measurements of pulsed Gaussian-beam spot sizes. *Opt. Lett.* **1982**, *7*, 196–198. [CrossRef] [PubMed]
36. Sanner, N.; Utéza, O.; Bussiere, B.; Coustillier, G.; Leray, A.; Itina, T.; Sentis, M. Measurement of femtosecond laser-induced damage and ablation thresholds in dielectrics. *Appl. Phys. A* **2009**, *94*, 889–897. [CrossRef]
37. Schott, A.G. *Technical Safety Information N-ZK7*, version 5; Schott AG: Mainz, Germany, 2015; pp. 1–7.
38. Brückner, S.; Rösner, S.; Gerhard, C.; Wieneke, S.; Viöl, W. Plasma-based ionisation spectroscopy for material analysis. *Mater. Test.* **2011**, *53*, 639–642. [CrossRef]
39. Gerhard, C.; Roux, S.; Brückner, S.; Wieneke, S.; Viöl, W. Low-temperature atmospheric pressure argon plasma treatment and hybrid laser-plasma ablation of barite crown and heavy flint glass. *Appl. Opt.* **2012**, *51*, 3847–3852. [CrossRef] [PubMed]
40. Gerhard, C.; Weihs, T.; Luca, A.; Wieneke, S.; Viöl, W. Polishing of optical media by dielectric barrier discharge inert gas plasma at atmospheric pressure. *J. Eur. Opt. Soc. Rapid Publ.* **2013**, *8*, 13081. [CrossRef]
41. Gredner, A.; Gerhard, C.; Wieneke, S.; Schmidt, K.; Viöl, W. Increase in generation of poly-crystalline silicon by atmospheric pressure plasma-assisted excimer laser annealing. *J. Mater. Sci. Eng. B* **2013**, *3*, 346–351.
42. Perry, M.D.; Stuart, B.C.; Banks, P.S.; Feit, M.D.; Yanovsky, V.; Rubenchik, A.M. Ultrashort-pulse laser machining of dielectric materials. *J. Appl. Phys.* **1999**, *85*, 6803–6810. [CrossRef]
43. Yang, L.; Yuan, X.D.; Deng, H.X.; Xiang, X.; Zheng, W.G.; He, S.B.; Jiang, Y.; Lv, H.B.; Ye, L.; Wang, H.J.; et al. Influence of ambient temperature on nanosecond and picosecond laser-induced bulk damage of fused silica. *Adv. Cond. Matter Phys.* **2014**, *2014*, 308918. [CrossRef]
44. Uteza, O.; Bussière, B.; Canova, F.; Chambaret, J.-P.; Delaporte, P.; Itina, T.; Sentis, M. Laser-induced damage threshold of sapphire in nanosecond, picosecond and femtosecond regimes. *Appl. Surf. Sci.* **2007**, *254*, 799–803. [CrossRef]
45. Gallais, L.; Mangote, B.; Zerrad, M.; Commandré, M.; Melninkaitis, A.; Mirauskas, J.; Jeskevic, M.; Sirutkaitis, V. Laser-induced damage of hafnia coatings as a function of pulse duration in the femtosecond to nanosecond range. *Appl. Opt.* **2011**, *50*, C178–C187. [CrossRef] [PubMed]
46. Kong, F.; Jin, Y.; Huang, H.; Zhang, H.; Liu, S.; He, H. Laser-induced damage of multilayer dielectric gratings with picosecond laser pulses under vacuum and air. *Opt. Laser Technol.* **2015**, *73*, 39–43. [CrossRef]
47. Rogov, V.V.; Rublev, N.D.; Krotenko, T.L.; Troyan, A.V. A study of intensity of tribochemical contact interaction between a polishing compound and sapphire in machining. *J. Superhard Mater.* **2008**, *30*, 273–275. [CrossRef]
48. Larruquert, J.I.; Pérez-Marín, A.P.; García-Cortés, S.; de Marcos, L.R.; Aznárez, J.A.; Méndez, J.A. Self-consistent optical constants of SiC thin films. *J. Opt. Soc. Am. A* **2011**, *28*, 2340–2345. [CrossRef] [PubMed]

49. Otanicar, T.P.; Phelan, P.E.; Golden, J.S. Optical properties of liquids for direct absorption solar thermal energy systems. *Sol. Energy* **2009**, *83*, 969–977. [CrossRef]
50. Wang, K.; Wen, W.; Wang, Y.; Wang, K.; He, J.; Wang, J.; Zhai, P.; Yang, Y.; Qiu, P. Order-of-magnitude multiphoton signal enhancement based on characterization of absorption spectra of immersion oils at the 1700-nm window. *Opt. Express* **2017**, *25*, 5909–5916. [CrossRef] [PubMed]
51. Zawilski, K.T.; Setzler, S.D.; Schunemann, P.G.; Pollak, T.M. Increasing the laser-induced damage threshold of single-crystal $ZnGeP_2$. *J. Opt. Soc. Am. B* **2006**, *23*, 2310–2316. [CrossRef]
52. Baravian, G.; Chaleix, D.; Choquet, P.; Nauche, P.L.; Puech, V.; Rozoy, M. Oil removal from iron surfaces by atmospheric-pressure barrier discharges. *Surf. Coat. Technol.* **1999**, *115*, 66–69. [CrossRef]
53. Swain, J.E.; Lowdermilk, W.H.; Milam, D. Raising the surface damage threshold of neutral solution processed BK-7 by pulsed laser irradiation. *Nat. Bur. Stand. Spec. Publ.* **1982**, *669*, 292–295.
54. Logothetis, E.M.; Hartman, P.L. Laser-induced electron emission from solids: Many-photon photoelectric effects and thermionic emission. *Phys. Rev.* **1969**, *187*, 460–474. [CrossRef]
55. Schubert, I. *Wissensspeicher Feinoptik*, 17th ed.; I. Schubert: Apolda, Germany, 2017; pp. 78–90, ISBN 978-3-00-046972-5. (In German)
56. Swain, M.V.; Metras, J.C.; Guillemet, C.G. A deformation and fracture mechanics approach to the scoring and breaking of glass. *J. Non-Cryst. Solids* **1980**, *38–39*, 445–450. [CrossRef]
57. Smirnov, M.I.; Spiridonov, Y.A.; Karapetyan, A.R. Modern sheet-glass cutting technologies. *Glass. Ceram.* **2011**, *68*, 6–10. [CrossRef]
58. Evans, C.J.; Paul, E.; Dornfeld, D.; Lucca, D.A.; Byrne, G.; Tricard, M.; Klocke, F.; Dambon, O.; Mullany, B.A. Material removal mechanisms in lapping and polishing. *CIRP Ann.-Manuf. Technol.* **2003**, *52*, 611–633. [CrossRef]
59. Cumbo, M.J.; Jacobs, S.D. Determination of near-surface forces in optical polishing using atomic force microscopy. *Nanotechnology* **1994**, *5*, 70–79. [CrossRef]
60. Sakata, H. Etude ellipsométrique du mécanisme fondamental de polissage du verre. *Jpn. J. Appl. Phys.* **1973**, *12*, 173–181. [CrossRef]

© 2018 by the authors. Licensee MDPI, Basel, Switzerland. This article is an open access article distributed under the terms and conditions of the Creative Commons Attribution (CC BY) license (http://creativecommons.org/licenses/by/4.0/).